ICANS IX

INTERNATIONAL COLLABORATION ON ADVANCED NEUTRON SOURCES

22-26 September, 1986

THE ROTATING ANALYSER CRYSTAL SPECTROMETER ROTAX

Holger Tietze and Reinhart Geick

University of Würzburg, Röntgenring 8, D-8700 Würzburg, West-Germany

Abstract

The rotating analyser crystal spectrometer (ROTAX) is an improved version of an inverted geometry TOF-X spectrometer, where the user has got the choice of different types of scans. By means of a non-uniformly rotating analyser, a flexibility of the spectrometer will be achieved which is intermediate between the crystal analyser time-of-flight spectrometers like MAX and Constant-Q and the triple axis spectrometer (TAS). In this paper we discuss the possibility of a proper constant-$\vec{Q}$ scan with ROTAX, in addition to constant-$\hbar\omega$ and constant-$\vec{Q}/|Q|$ scans.

Introduction

The instrument most commonly used for studying collective excitations in solids like phonons, magnons etc. is the triple axis spectrometer (TAS)[1-4], especially at continuous neutron sources. However, for pulsed spallation neutron sources the question arises how a spectrometer can be constructed which is adapted to the time structure of the neutron pulses and still has the same flexibility and versality as the TAS. Two different types of spectrometers have been developed so far for coherent inelastic scattering at pulsed sources, namely the multi-analyser crystal spectrometer (MAX in Japan[5] and PRISMA in UK[6] and the Constant-Q spectrometer in UK[7] and in USA[8]).

In a previous paper[9] we have outlined the basic ideas of our proposal for a new type of instrument for coherent elastic and inelastic scattering from single crystals at pulsed neutron sources. While the TAS employs two Bragg reflections, one at the monochromator and the other at the analyser, the instruments at pulsed sources considered here are time-of-flight crystal analyser spectrometers with inverted geometry. For our proposed spectrometer, we have shown[9] that its flexibility and versality is intermediate between the TAS, on one hand, and the MAX and Constant-Q spectrometer, on the other hand. That can be achieved by a non-uniform rotation of the analyser crystal which means an optimum adaption to the pulse structure of the source and a most economic use of the available neutrons (multiplex advantage). The non-uniform rotation of the analyser is, within the limits of feasibility, arbitrarily progammable according to the user's choice, e.g. constant-$\hbar\omega$ or constant-$\vec{Q}/|Q|$ scan. In order to have the same flexibility as with TAS, e.g. the proper constant-$\vec{Q}$ scan, it would be necessary to rotate non-uniformly not only the analyser but also the sample as will be shown in detail below.

Scans with ROTAX

ROTAX can be understood from the basic scattering equations, which govern the scattering triangle. For all instruments with inverted geometry at a pulsed source, the wavevector k_i and energy E_i of the incoming neutrons depend on the incident flight time t_i between moderator and sample (cf. fig. 1). Our basic approach is then to express all other quantities of the scattering process like the wavevector k_f of the scattered neutrons or the analyser Bragg angle θ_A as functions of t_i. k_f and θ_A are connected by Bragg's law

$$k_f(t_i) = \pi / d_A \sin \theta_A(t_i). \qquad (1)$$

The flight time between sample and analyser is given by

$$t_a(t_i) = \frac{L_a}{v_f(t_i)} = \frac{m}{\hbar} \frac{L_a}{k_f(t_i)} \qquad (2)$$

Equations (1) and (2) have to be solved simultaneously

$$\sin \theta_A(t_i) = \frac{h}{2m\, L_a\, d_A}\, t_a(t_i). \qquad (3)$$

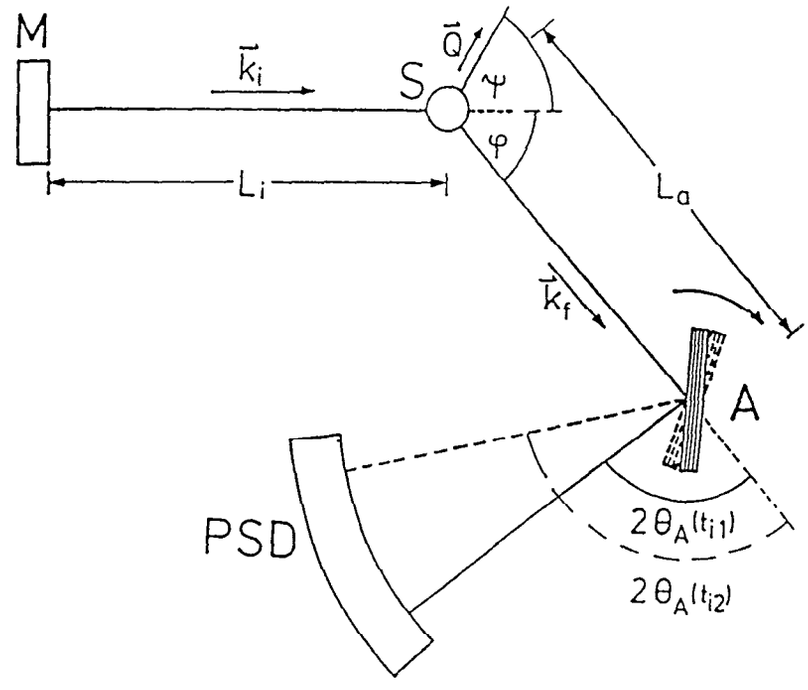

fig. 1
Schematic drawing of the rotating analyser crystal spectrometer (ROTAX); moderator (M), sample (S), analyser (A), detector (PSD).

From our previous study[9] it turned out that, in addition to the scattering angle ϕ, one more scattering parameter can be chosen constant, i.e. independent of t_i. Hence, the experimenter can choose between various types of special scans, e.g. const.-$\hbar\omega$ or const.-$\vec{Q}/|Q|$ or const.-$|\vec{Q}|$ scan. In order to perform such a special scan the anaylser angle θ_A (eq. 3) has to be varied according to the appropriate function $t_a(t_i)$ depending on the type of scan. $t_a(t_i)$ can be determined from the scattering triangle, which connects k_i with k_f.

We obtain

$$t_a = L_a \left[\left(\frac{L_i}{t_i} \right)^2 - \frac{2}{m} \hbar\omega \right]^{-1/2} \qquad (4a)$$

$$t_a = t_i \frac{L_a}{L_i} \frac{\sin(\psi + \phi)}{\sin \psi} \qquad (4b)$$

for the const.-$\hbar\omega$ and const.-ψ scan respectively, where ψ is the sample orientation angle (cf. fig. 1) defining the direction of $\vec{Q}/|Q|$ with respect to the crystal axes of the sample. The resulting curves for the analyser setting are presented in fig. 2, from which the rotation speed can be deduced.

As obvious from eqs. (3) and (4a) the analyser rotation is almost uniform ($\nu = 19$ Hz) for $\hbar\omega = 0$ as long as the $\sin^{-1}$-function is almost linear ($\theta_A < 30°$). For $\hbar\omega > 0$, the curves in fig. 2a exhibit an angular velocity for the analyser increasing from its starting value for $t_i = 1$ msec. In order to keep the angular velocity within reasonable limits the measurement and the appropriately programmed non-uniform rotation of the analyser should be terminated at about $\theta_A \approx 30°$ or for 2 msec $< t_i <$ 4 msec. For $\hbar\omega < 0$, the curves in fig. 2a show a decreasing angular velocity and the measurement can be extended, in principle, over a wider range. In all cases (const.-$\hbar\omega$ and const.-ψ), the time between the termination of the measurement (rotation of θ_A according to the curves in fig. 2) and the next neutron pulse has to be used to return the analyser back to its original position either by back-rotation or by half or full circle rotation (180° or 360°). Since the derivatives of the curves in fig. 2 correspond mostly to frequencies near to 25 Hz, a total rotation of the analyser by 180° per cycle seems to be preferable at the British spallation source ISIS with a neutron pulse repetition frequency of $\nu = 50$ Hz.

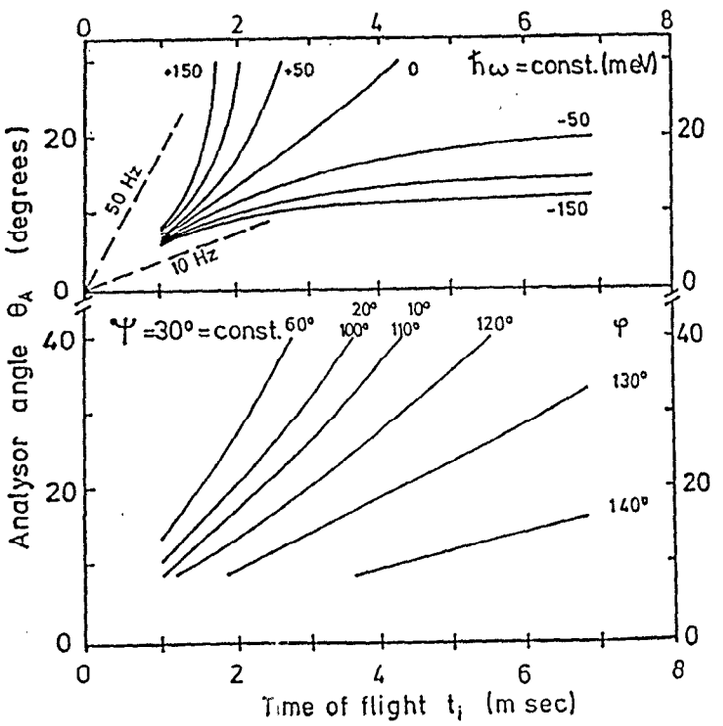

fig. 2
Analyser Bragg angle θ_A as a function of flight time t_i between moderator and sample for ROTAX. (a) const.-$\hbar\omega$ scans for various energy transfers $\hbar\omega$; (b) const.-ψ scans for $\psi = 30°$ and for various scattering angles ϕ.

For a const.-ψ scan eq. (4b) reveals immediately that the non-uniformity of the analyser rotation is smaller in this case as compared to the const.-$\hbar\omega$ scan, where the essential non-linearity originates from the square-root in the denominator of eq. (4a). These properties are clearly demonstrated by the curves of θ_A versus t_i for ψ = const. = 30° and for various scattering angles ϕ in fig. 2b. A further difference to the case $\hbar\omega$ = const. is that θ_A depends in a non-monotonous way on $\sin(\psi+\phi)$. In fact, an angle ϕ_1 and an associated angle $\phi_2 = \pi - 2\psi - \phi_1$ generate the same curve $\theta_A(t_i)$. For positive energy transfer $\hbar\omega > 0$ which means $\phi < 120°$ for ψ = 30° the derivatives of the curves in fig. 2b also correspond to frequencies between 10 and 50 Hz. That means again a preferable total rotation of the analyser of 180° per cycle. Due to the smaller non-linearity of the curves, the const.-ψ scans may be extended to analyser Bragg angles up to $\theta_A \leq 45°$ using the neutrons of a pulse arriving between 1 msec $< t_i <$ 4 msec at the sample.

As already mentioned, many other paths for the TOF scan in Q-space may be thought of. But not all of them will be feasible. An example for such a case is a TOF scan where the magnitude of Q is kept constant. For $|\vec{Q}|=Q=$const., we obtain

$$Q^2 = k_i^2 + k_f^2 - 2\, k_i\, k_f \cos\phi \,. \qquad (5)$$

The possible scattering triangles according to eq. (5) are illustrated in fig. 3. It is evident that this type of scan requires $k_i \leq Q/\sin\phi$. In general eq. (5) yields two solutions k_f^+ and k_f^-, but only values $k_f > 0$ are physically meaningful (cf. tab. 1 with the different ranges for energy loss or gain of the neutrons).

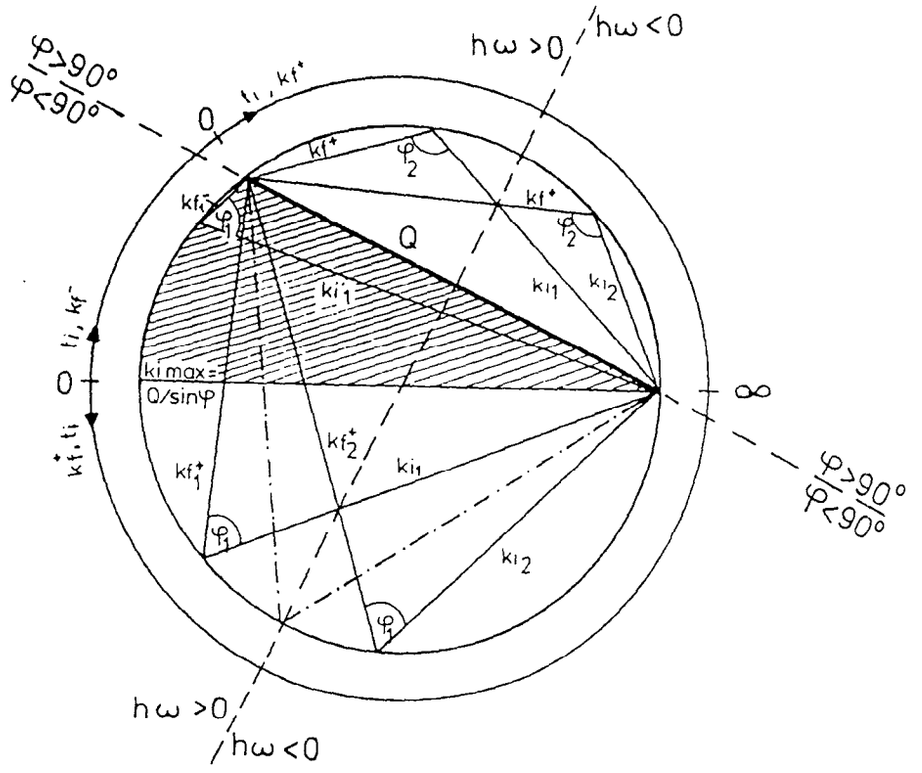

fig. 3
Scattering triangle for const.-$\vec{Q}$ scans with ROTAX. Equivalent solutions for different spectrometer configurations are illustrated for energy gain or loss of the neutrons and for the different types of solutions k_f^- (shaded area) and k_f^+ for the cases discussed in tab. 1.

Tab. 1: Solutions of eq. (5) for k_f^+ and k_f^- yielding energy gain ($\hbar\omega<0$) or energy loss ($\hbar\omega>0$) of the neutrons.

+ Solution: $k_f^+ = k_i \cos\phi + \sqrt{Q^2 - (k_i \sin\phi)^2}$

	$0 \leq \phi \leq 90°$	$90° \leq \phi \leq 180°$
$\hbar\omega \geq 0$	$\frac{Q}{2\sin(\phi/2)} \leq k_i \leq \frac{Q}{\sin\phi}$	$\frac{Q}{2\sin(\phi/2)} \leq k_i \leq Q$
$\hbar\omega \leq 0$	$0 \leq k_i \leq \frac{Q}{2\sin(\phi/2)}$	$0 \leq k_i \leq \frac{Q}{2\sin(\phi/2)}$

− Solution: $k_f^- = k_i \cos\phi - \sqrt{Q^2 - (k_i \sin\phi)^2}$

	$0 \leq \phi \leq 90°$	$90° \leq \phi \leq 180°$
$\hbar\omega \geq 0$	$Q \leq k_i \leq \frac{Q}{\sin\phi}$	———
$\hbar\omega \leq 0$	———	———

The flight time t_a between sample and analyser immediately reads

$$t_a(t_i) = L_a \left[\frac{L_i}{t_i} \cos\phi \pm \sqrt{\left(\frac{\hbar Q}{m}\right)^2 - \left(\frac{L_i \sin\phi}{t_i}\right)^2} \right]^{-1} \qquad (6)$$

and the corresponding values for θ_A are sketched in fig. 4 for $|Q| = 5\ \text{Å}^{-1} = \text{const}$. The curves for both solutions $\theta_A(k_f^+)$ and $\theta_A(k_f^-)$ start at the common point (+) with infinite rotation speed $d\theta_A/dt_i$. For smaller values of t_i (larger values of k_i) the argument of the square-root in eq. (6) is negative. The curves for $\theta_A(k_f^+)$ show that the analyser has to be accelerated to a rather high rotation frequency and then, starting somewhat away from the common point (+), to be slowed down very rapidly until the line of zero energy transfer (second broken line in fig. 4) is reached. Then, the curves approach an asymptotic value $\theta_A = \text{const}$. (MAX spectrometer!) similar to fig. 2a. Solution $\theta_A(k_f^-)$ shows a deceleration from the common point (+) turning to an acceleration then at very high rotation speeds. In general, the non-uniform rotation of the analyser according to this const.-$|Q|$ scan (cf. fig. 4) seems not to be feasible with the drastic deceleration of the rotation to nearly complete stop and then with the subsequent relatively high angular acceleration to complete the cycle. Only for high scattering angles $\phi \geq 120°$ the analyser rotation might be technically feasible.

It is noteworthy to look at the total time-of-flight for this type of const.-$|Q|$ scan. The total time-of-flight t_o is the time of arrival at the detector. It is obvious from eq. (5) that one possible solution is $k_i = Q$ with $k_f = 0$, not depending on ϕ. That would mean a full stop of the neutrons at the sample yielding an infinite total time-of-flight, of course. This is being illustrated in

fig. 5, where the total TOF t_o is plotted versus the incident TOF t_i for various scattering angles ϕ. Again , the common point (+) of both the solutions k_f^+, k_f^- is characterised by the minimum value of t_i. Please remark, that the slope of the curves $t_o(t_i)$ depend on the special kind of the solution k_f^+, k_f^- (cf. tab. 1). Apart from the strange properties of $t_o(t_i)$ for $\phi < 90°$, the curves for $\phi > 90°$ do not reveal an unambigous value of t_o as a function of t_i, i.e. there exist neutrons which overtake previously started neutrons of the same pulse in the secondary part of the spectrometer. For practical use the monotonous ascending branches of $t_o(t_i)$ are applicable only. Hence, the neutrons with higher energies and corresponding flight times $t_i < t_{i,min}$ have to be suppressed physically with an auxiliary chopper between moderator and sample.

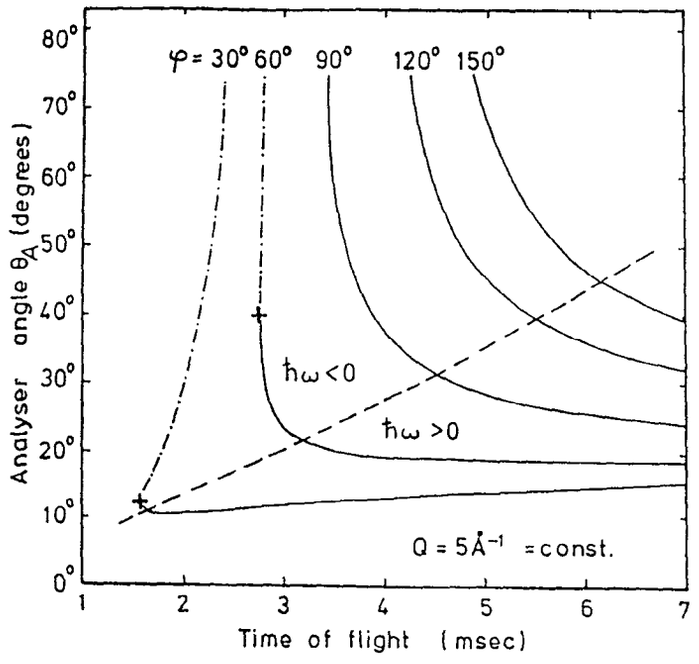

fig. 4
Analyser Bragg angle θ_A versus flight time t_i for a const.-$|Q|$ scan at various scattering angles ϕ. Both solutions for k_f^- (dash-point) and k_f^+ (solid lines) starting at their common points (+) are illustrated and the change of energy transfer is indicated (broken line).

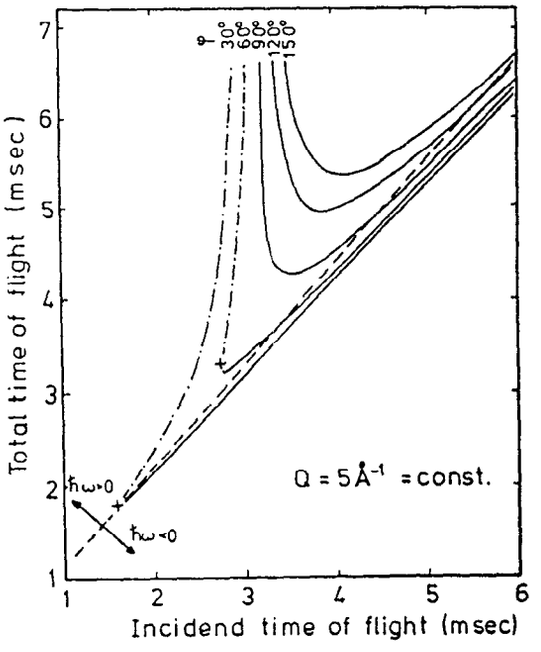

fig. 5
Total time-of-flight t_o between moderator and detector versus incident time-of-flight t_i between moderator and sample. Again dash-points denote solutions of k_f^-, solid curves solutions of k_f^+, (+) common starting points and the brocken line the change of the sign of $\hbar\omega$.

If all these limitations previously discussed are met, the const.-|Q| scan can be performed as a proper const.-$\vec{Q}$ scan if also the sample is non-uniformly rotated, corresponding to

$$\operatorname{tg}\psi(t_i) = \frac{k_f \sin\phi}{k_i - k_f\cos\phi} = \frac{k_i \sin\phi\cos\phi \pm \sin\phi\sqrt{Q^2 - (k_i\sin\phi)^2}}{k_i \sin^2\phi \mp \cos\phi\sqrt{Q^2 - (k_i\sin\phi)^2}} \quad . \qquad (7)$$

Eq. (7) is illustrated in fig. 6 and means that $\psi(t_i)$ varies just in such a way that the direction of $\vec{Q}$ remains constant with respect to the crystal axes of the sample during one scan (cf. fig. 3).

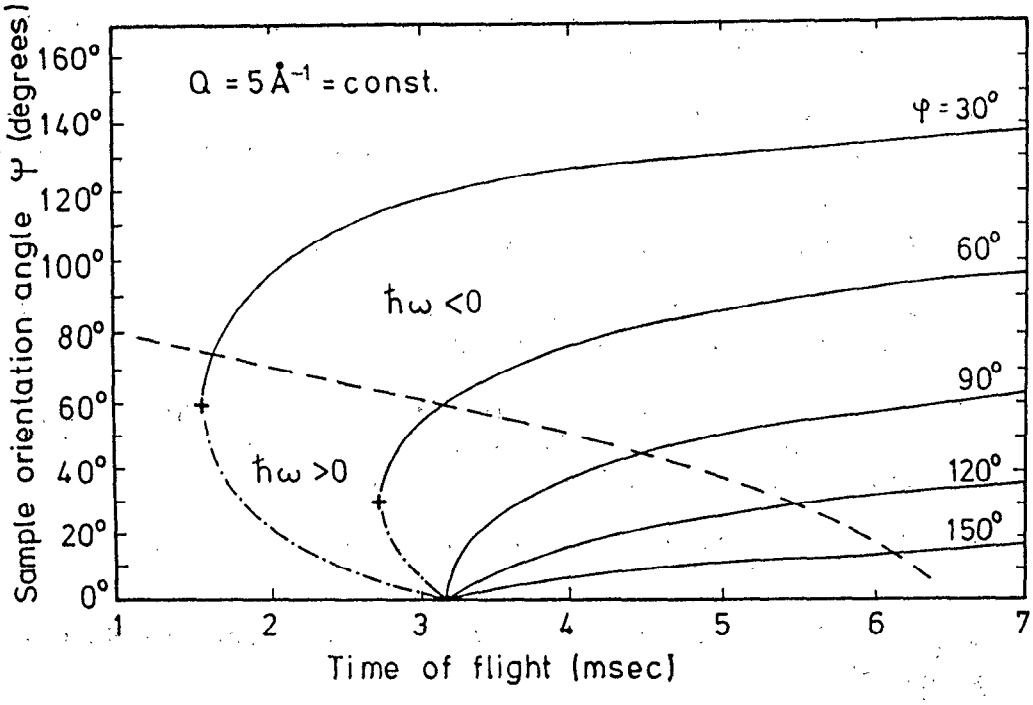

fig. 6
Sample orientation angle ψ versus incident time-of-flight t_i for various scattering angles ϕ and both solutions of k_f^- (dash-points) and k_f^+ (solid).

Conclusions

i) It has been shown, that in principle ROTAX can provide widely variable const.-$\hbar\omega$ and const.-ψ scans, as well as severely limited const.-$\vec{Q}$ scans.

ii) const.-$\hbar\omega$ and const.-ψ scans are rather easy to perform, because $t_o(t_i)$ is a monotonous function and $\theta_A(t_i)$ provides fesible values.

iii) The flexibility of ROTAX ensures that in case of phonon measurements their polarisation can be taken care of.

iv) The limitations for a proper const.-$\vec{Q}$ scan are that the sample has to be rotated non-uniformly and in phase with the pulse structure and the analyser rotation. Further, this mode of operation has to be restricted to scattering angles $\phi \gtrsim 120°$, which obviously excludes measurements of magnetic excitations.

Acknowledgements

We would like to thank Dr. J. M. Carpenter (ANL) and Dr. C. G. Windsor (RAL) for valuable discussions. The financial support of the BMFT, Förderkennzeichen 03-Ge 1 Wue-6, is gratefully acknowledged.

References

[1] G. Dolling, in "Dynamical Properties of Solids", ed. by G. K. Horton and A. A. Maradudin (North Holland, Amsterdam, 1974), Vol. 1, p. 541-629.

[2] S. W. Lovesey and T. Springer (eds.): Dynamics of Solids and Liquids by Neutron Scattering, Topics in Current Physics, Vol. 3 (Springer, Berlin-Heidelberg-New York, 1977).

[3] B. Dorner: Coherent Inelastic Neutron Scattering in Lattice Dynamics, Springer Tracts in Modern Physics, Vol. 93 (Springer, Berlin-Heidelberg-New York, 1982).

[4] R. Pynn, Rev. Sci. Instr. 55 (1984) 837.

[5] K. Tajima, Y. Ishikawa, K. Kanai, C. G. Windsor and S. Tomiyoshi, Nucl. Instr. and Meth. 201 (1982) 491

[6] C. Andreani, F. Cilloco, C. Petrillo, F. Sacchetti and C. G. Windsor, Rapporto Interno 1985/4 dell'Instituto di Struttura della Materia del CNR, Frascati (Italia), and priv. commun.

[7] C. G. Windsor, R. K. Heenan, B. Boland and D. Mildner, Nucl. Instr. and Meth. 151 (1978) 477

[8] R. A. Robinson, R. Pynn and J. Eckert, subm. to Nucl. Instr. and Meth. (1985).

[9] R. Geick and H. Tietze, Nucl. Instr. and Meth. A 249 (1986) 325.